SciMedCentral

JSM Nanotechnology & Nanomedicine

Research Article

Fructose Chitosan Based Self-Assembled Nanoparticles for Sustained Release of Vitamins and Steroids

Javier Pérez Quiñones[1]*, Oliver Brüggemann[1], and Carlos Peniche Covas[2]

[1]*Institute of Polymer Chemistry, Johannes Kepler University Linz, Austria*

[2]*Center of Biomaterials, University of Havana, Cuba*

***Corresponding author**

Javier Pérez Quiñones, Institute of Polymer Chemistry, Johannes Kepler University Linz, Altenberger Straße 69, 4040 Linz, Austria, Tel: 4368120399376; Email: javenator@gmail.com

Submitted: 23 October 2017

Accepted: 06 November 2017

Published: 09 November 2017

ISSN: 2334-1815

Keywords

- Sustained release; Fructose chitosan; Self-assembled nanoparticles; Steroids; Vitamins

Abstract

Synthetic fructose chitosan (FC) was linked to DL-α-tocopherol, ergocalciferol, diosgenin and two synthetic analogues of brassinosteroids via a succinate linker by carbodiimide coupling in solution. Conjugates with substitution degrees of 5.5 to 39.0% were obtained and used for the sustained release of agrochemicals and potential anticancer drugs. FTIR and proton NMR spectroscopies confirmed the hydrophobic modification of fructose chitosan. Differential scanning calorimetry and wide-angle X-ray diffraction studies of prepared FC conjugates are also presented. The amphiphilic FC-vitamin and FC-steroid conjugates self-assembled in aqueous medium as stable and positively charged nanoparticles of 165 to 213 nm with +30 to +54.2 mV, as revealed using dynamic light scattering. Almost spherical nanoparticles of 40 to 65 nm in dried state were observed by SEM and TEM. Sustained release of linked vitamins and steroids in phosphate buffer saline solution at pH 6.0 was observed over 96 h, while almost constant release rates were perceived during the first 7 to 8 h. Brassinosteroid-N-modified fructose chitosan nanoparticles showed good agrochemical activity. These results indicated that the obtained nanoparticles might be potential drug delivery system of vitamins and steroids for anticancer and agrochemical applications.

INTRODUCTION

Chitosan is a natural and linear copolymer, consisting of randomly distributed β (1 → 4) linked D-glucosamine units and some proportion of N-acetyl-D-glucosamine units. It is obtained by extensive deacetylation of chitin [1]. Chitosan is considered a biomaterial with excellent properties and benefits for animals and humans [2,3]. It also increases photosynthesis, promotes and enhances plant growth, stimulates nutrient uptake, increases germination of seeds and sprouting, boosts plant vigor and stimulates defense mechanisms in plants [4]. It is capable of enhancing the transport of polar drugs trough epithelial membranes; but its application in medicine and the pharmaceutical field is limited due to water solubility restricted to acidic pH and short time stability of self-aggregated chitosan conjugates in solution [5]. Some chitosan derivatives overcome these limitations, still showing good biocompatibility (i.e. glycol chitosan, fructose chitosan) [6,7]. Fructose chitosan (FC) is prepared by Maillard reaction (reductive amination) between fructose and chitosan [7,8]. It has been employed for hepatocyte growth and liver injury treatment [9].

Vitamin D2 (ergocalciferol) and vitamin E (DL-α-tocopherol as main constituent) are lipophilic vitamins with important effects on animals and humans. Ergocalciferol is involved in skeleton development [10], while vitamin E is a potent antioxidant and protective agent of cell membranes and lipid peroxidation process [11,12]. Anticancer activity of ergocalciferol and α-tocopherol has been thoroughly studied [13,14]. On the other hand, diosgenin and some saponins containing it exhibit important antitumor and anticancer properties [15]. Together with some natural and synthetic brassinosteroids, diosgenin also presents antiproliferative, antiherpetic and anti-HIV activity in animals and humans [16]. Additionally, diosgenin is the main substrate in chemical synthesis of the Cuban synthetic analogue of brassinosteroid DI31 [17], used as commercial agrochemical Biobras-16. It is known that Biobras-16 promotes vegetal growth with increases in harvest of 5 to 25%, while protecting the crops of abiotic and biotic stress [18].

Brassinosteroids are steroidal phytohormones widely found in reproductive and vegetative plant tissues. They are involved in the defense mechanisms of plants, growth, reproduction and several physiological processes [19]. Its benefits in plants include protection against fungi and bacterial attacks, dryness, salinity and extreme temperatures [20]. However, plants metabolize fast the synthetic brassinosteroids used as agrochemicals, limiting their benefits [21]. The brassinosteroids and lipophilic vitamins E and D2 are hydrophobic compounds with very low aqueous solubility, and therefore require chemical modifications or to be included in adequate formulations for practical use. In this sense, chitosan was covalently modified with diosgenin hemiesters for controlled release of diosgenin as a proof of concept [22]. However, obtained chitosan-diosgenin conjugates were not

suitable for pharmaceutical applications because the limited solubility in aqueous medium. That is why the choice of water-soluble chitosan derivatives for preparation of amphiphilic chitosan-vitamin and chitosan-steroid conjugates capable of self-assembly in aqueous medium as stable nanocarriers is appealing.

The synthesis of tocopherol-, ergocalciferol- and steroid-N-modified fructose chitosan conjugates will allow accomplishing its controlled delivery, overcoming their low aqueous solubility and combining their positive effects on plants, humans and animals with the biocompatibility, antioxidant and microbicidal properties of the chitosan matrix [2,3,23]. In the current work, we synthesized novel FC-vitamin and FC-steroid conjugates by amidation of fructose chitosan with tocopherol hemisuccinate, ergocalciferol hemisuccinate and steroid hemisuccinates. The prepared FC conjugates, which self-assemble as nanoparticles in aqueous solution, were intended for *in vitro* delivery of linked vitamins and steroids mediated by hydrolysis of ester bond of hemisuccinate linker. Preliminary studies of agrochemical activity of synthesized FC-brassinosteroid conjugates towards radish (*Raphanus sativus*) were also conducted.

EXPERIMENTAL

Materials

Chitosan (acetylation degree, DA = 19.8% determined by ^{1}H-NMR, Mw= 4.3×10^5) was purchased from Sigma-Aldrich. Hemisuccinates of DL-α-tocopherol, ergocalciferol, diosgenin and two synthetic analogues of brassinosteroids with agrochemical activity (DI-31 and S7), were synthesized by base-catalyzed traditional esterification in pyridine with succinic anhydride [24]. Fructose chitosan was prepared by the Maillard reaction of commercial chitosan (1%, w/v) with fructose (1%, w/v) in 0.2 M aqueous acetic acid solution at 65 °C, affording a substitution degree of 5.6 mol-% by elemental analysis (19.8 acetyl molecules and 5.6 fructose molecules by 100 molecules of chitosan) [7,8]. Diosgenin and the synthetic analogues of brassinosteroids (DI-31 and S-7) were supplied by the Center of Natural Products of the University of Havana. Solvents and reagents employed were purchased from Sigma-Aldrich and used without further purification.

The structures of DL-α-tocopherol hemisuccinyl fructose chitosan (FC-MSToc), ergocalciferol hemisuccinyl fructose chitosan (FC-MSVitD2), diosgenin hemisuccinyl fructose chitosan (FC-MSD), DI-31 hemisuccinyl fructose chitosan (FC-MSDI31), S7 hemisuccinyl fructose chitosan (FC-MSS7) conjugates and fructose chitosan (FC) are shown in Figure 1.

Preparation of hydrophobically-modified FC nanoparticles

Synthesis of hydrophobically-modified FC-vitamin and FC-steroid conjugates: 210 mg (ca. 0.5 mmol) of fructose chitosan were dissolved in 8 mL of bi-distilled water and diluted with 24 mL of anhydrous ethanol. 38 mg (0.20 mmol) of 1-ethyl-3-(3-dimethylaminopropyl) carbodiimide hydrochloride (EDC) and 23 mg (0.20 mmol) of N-hydroxisuccinimide were added, and the mixture was stirred until solution clearance. 75-90 mg (0.15 mmol) of hemisuccinate of DL-α-tocopherol, ergocalciferol, diosgenin, DI31 or S7 were dissolved in 32 mL of ethanol/water mixture (85:15, v/v) and slowly added with stirring to the FC solution. The reaction mixture was stirred 72 h at room temperature and dialyzed (Spectra/Por 1, MWCO 6 000-8 000 Da) against ethanol/water mixture (90:10, 66:33, 50:50 and 0:100, v/v), each one for 2 days with 16 exchanges. The dialyzed solution was lyophilized affording white or slightly yellow, cotton wool-like products.

Preparation of the self-assembled FC nanoparticles: The synthesized hydrophobically-modified FC conjugates were able to form nanoparticles in aqueous medium after stirring overnight and probe tip sonication. To this end, the FC-vitamin and FC-steroid conjugates (ca. 0.5-2.0 mg mL^{-1}) were stirred overnight at 100 rpm in bi-distilled water or phosphate buffered saline solution (PBS, pH 7.4), as required. The solutions were probe tip sonicated (Branson Sonifier W-250, Heinemann, Germany) at 20 W for 2 min in an ice bath. The sonication step was repeated five times. The pulse function was pulsed on 8.0 s and pulsed off 2.0 s [5].

Characterization

The synthesized FC-vitamin and FC-steroid conjugates were characterized by FTIR spectroscopy using a Perkin-Elmer 1720 FTIR spectrophotometer (Perkin-Elmer Corporation, Norwalk, Connecticut, USA) with 32 scans and 4 cm^{-1} resolution. Samples were prepared by the KBr pellet method. Elemental analyses were performed on a Vario MicroCube Analyzer (Elementar Analysensysteme, Germany) with burning temperature of 1150 °C. The ^{1}H-NMR spectra were recorded with an OXFORD NMR AS400 (VARIAN) spectrometer (Varian, Palo Alto, CA, USA) operating at 400.46 MHz for proton at 25 °C with concentrations ca. 8-25 mg mL^{-1} in d2-water and d4-acetic acid/d2-water (25%, v/v) and analyzed with the VNMRJ software, version 2.2. Wide-angle X-ray diffraction (WAXD) analysis of the powered samples was performed using a Rigaku SmartLab X-Ray diffractometer (Rigaku, Tokyo, Japan) with Cu K_α radiation (40 kV, 30 mA, λ = 0.15418 nm), data collected at a scan rate of 1 ° min^{-1} with a scan angle from 4 to 50°. Calorimetric curves were obtained with a Perkin-Elmer Differential Scanning Calorimeter Pyris 1 (Perkin-Elmer Instrument Inc., Boston, MA, USA) and analyzed with the Pyris 1 software (version 6.0.0.033). Differential scanning calorimetry (DSC) studies were conducted using sample weights of ca. 5 mg, under nitrogen dynamic flow of 20.0 mL min^{-1} and a heating-cooling rate of 10 °C min^{-1} [22]. Samples were deposited in aluminum capsules and hermetically sealed. Indium was used to calibrate the instrument. Enthalpy (ΔH in J/g dry weight) and peak temperature were computed automatically. Samples were heated and cooled from -30 to 300 °C. Dynamic light scattering (DLS) studies were performed using Zetasizer Nano ZS (Malvern Instruments, Malvern, UK) at 25 °C to obtain the particle size and zeta potential. The size and morphology of dried FC-vitamin and FC-steroid nanoparticles were studied by transmission electron microscopy (TEM) with a Philips CM20 (Philips, Amsterdam, Netherlands) operating at 200 kV and scanning electron microscopy (SEM) with a Nova NanoSEM 600 (FEI, Hillsboro, Oregon, USA). Samples were stirred in bi-distilled water (ca. 1 mg mL^{-1}) 48 h and a drop was deposited on carbon plates. The excess solution was removed with filter paper and dried in air. The SEM samples were coated with gold. The TEM samples were negative stained with a drop of uranyl acetate solution (1 wt-%).

In vitro drug release studies

In vitro drug release of DL-α-tocopherol, ergocalciferol and steroids from FC-MSToc, FC-MSVitD2 or FC-steroid nanoparticles was studied by UV detection (Genesys 10 UV-Vis Spectrophotometer, Thermo Spectronic, Rochester, N.Y., USA) of the delivered DL-α-tocopherol at 292 nm, ergocalciferol at 265 nm or steroids (diosgenin at 280 nm, DI31 and S7 at 300 nm) in PBS at pH 6.0. 10 mg of FC-vitamin or FC-steroid nanoparticles dissolved in PBS solutions (5 mL) at pH 6 were placed in dialysis bag (Spectra/Por 4, MWCO 12 000-14 000 Da) and dialyzed against the release media (PBS pH 6, 40 mL) at 30 ˚C (FC-MSD, FC-MSDI31, FC-MSS7) or 37 ˚C (FC-MSToc, FC-MSVitD2) with constant agitation at 100 rpm. The entire media was removed at determined time intervals, and replaced with the same volume of fresh media. The amount of DL-α-tocopherol, ergocalciferol or steroids released was determined from a previously obtained UV calibration curve. These studies were conducted in triplicate for each sample.

Radish cotyledon test for agrochemical activity bioassay

The radish (*Raphanus sativus*) test was employed in order to assess plant growth activity. This bioassay consists of measuring the increased weight of the treated radish's cotyledons (auxin type activity). Briefly, radish seeds previously sanitized by sodium hypochlorite treatment were germinated on wet filter paper in dark at 25 ˚C, for 72 h [25]. Cotyledons were separated of hypocotyls and excess water was removed with filter paper. The cotyledons were weighted and treated with 5 mL of FC-MSDI31 or FC-MSS7 nanoparticles in water (10^{-1} to 10^{-7} mg mL^{-1}); DI31 or S7 solutions (10^{-1} to 10^{-7} mg mL^{-1}); fructose chitosan aqueous solution (10^{-1} to 10^{-7} mg mL^{-1}) or bi-distilled water (control). After 72 h, cotyledons were weighted again. These studies were performed in triplicate for each sample and concentration (10 cotyledons per each run).

RESULTS AND DISCUSSION

The hydrophobic modification of water soluble FC with hemisuccinates of vitamins and steroids via amidation in aqueous solution activated by carbodiimide coupling afforded FC-vitamin and FC-steroid conjugates with substitution degrees in DL-α-tocopherol of 39.0 mol-% (equivalent to a DL-α-tocopherol content of 44.0 wt-%), in ergocalciferol of 5.5 mol-% (equivalent to a 10.6 wt-% of ergocalciferol) and in steroids of 29 to 33 mol-% (FC-MSD 29 mol-%, for a content of 36.9 wt-% of diosgenin; FC-MSDI31 30 mol-%, for a content of 39.7 wt-% of DI31; FC-MSS7 33 mol-%, for a content of 42.3 wt-% of S7). The employed synthetic route involved mild and efficient amidation (ca. 65-80% yields relative to starting FC) of free primary amine groups of FC with vitamin or steroid hemisuccinates.

Synthesized FC-vitamin and FC-steroid conjugates formed self-assembled nanoparticles in aqueous solution with average particle sizes between 165 nm and 213 nm, due to their hydrophilic/hydrophobic moieties.

Characterization

Dynamic light scattering studies conducted in triplicate detected average hydrodynamic particle diameters in PBS solution of: 195 ± 6 nm with a polydispersity index (PDI, indication of the width of the overall distribution) of 0.39 ± 0.02 (FC-MSToc), 213 ± 3 nm with a PDI of 0.83 ± 0.02 (FC-MSVitD2), 205 ± 3 nm with a PDI of 0.25 ± 0.02 (FC-MSD), 199 ± 5 nm with a PDI of 0.43 ± 0.05 (FC-MSDI31) and 165 ± 4 nm with a PDI of 0.50 ± 0.04 (FC-MSS7). These FC nanoparticles were formed in aqueous medium with a 3 to 6 mol-% of aggregates with ca. 4.6 to 5.4 μm sizes. Zeta potential of the FC nanoparticles measured in bi-distilled water were: +32.5 ± 0.4 mV (FC-MSToc), +30 ± 3 mV (FC-MSVitD2), +40 ± 2 mV (FC-MSD), +54.2 ± 0.5 mV (FC-MSDI31) and +50.5 ± 0.3 mV (FC-MSS7). The relative high surface charges associated with zeta potential values over 30 mV, might provide colloidal stability in aqueous medium [26]. Experimentally, no significant differences in hydrodynamic parameters (hydrodynamic diameters and PDI) were observed after keeping the FC nanoparticles dispersions after 2 weeks of storage (data not shown).

Figure 2 shows the SEM and TEM images of dried tocopheryl-N-modified, ergocalciferol-N-modified and steroid-N-modified FC nanoparticles. The SEM micrographs showed almost spherical nanoparticles, while TEM images showed particles with 40-65 nm mean diameters. In this study, observed shrinkage of the FC nanoparticles upon drying was ca. 60 to 80%. Shrinkage of dried chitosan based nanoparticles of up to 80% was described for other amphiphilic chitosan-drug conjugates [27]. It might be due to that the nanoparticles are allowed to dry and dehydrate before electron microscopy imaging.

The FTIR spectra of FC-vitamin and FC-steroid conjugates are shown in Figure 3. The spectra of chitosan and fructose chitosan are also included for comparison. The IR spectrum of chitosan (Figure 3 (I) (a)) presented the characteristic absorption peaks at 2942-2784 cm^{-1} (aliphatic C-H stretching band), 1658 cm^{-1} (Amide 1) and 1597 cm^{-1} ($-NH_2$) bending and 1321 cm^{-1} (Amide III). Absorption peaks at 1154 cm^{-1} (antisymmetric stretching of the C-O-C bridge), 1082 and 1032 cm^{-1} (skeletal vibrations involving the C-O stretching) are due to its saccharide structure [28]. Fructose chitosan showed a quite similar IR spectrum (Figure 3(I) (b)), due to lack of additional functional groups compared to chitosan and low substitution degree with fructose (5.6 mol-%). On the other hand, the synthesized FC-vitamin and FC-steroid conjugates showed additional characteristic peaks. Thus, FC-MSToc conjugate (Figure 3 (I) (c)) exhibited C=O IR absorption at 1742 cm^{-1} (ester linkage) and an intense peak at 1557 cm^{-1} (Amide II band, N-H bending of amide groups formed between tocopheryl hemisuccinate and FC). Besides, the FTIR spectrum of FC-MSVitD2 (Figure 3 (I) (d)) showed the C=O absorption band at 1734 cm^{-1} (ester linkage) as a slight shoulder due to a low functionalization of chitosan matrix with ergocalciferol (5.5 mol-%), while an intense absorption band at 1560 cm^{-1} (Amide II band, N-H bending of amide formed between ergocalciferol hemisuccinate and FC) is also observed.

The IR spectrum of the FC-MSD conjugate (Figure 3 (II) (b)) presents an intense absorption band at 1734 cm^{-1} (C=O of ester linkage) and an intense band at 1557 cm^{-1} (Amide II band, N-H bending of amide linkage formed between diosgenin hemisuccinate and FC). The brassinosteroid-N-modified fructose chitosan IR spectra (Figure 3 (II) (c) and (d)) showed intense

ketone C=O absorptions at 1714 cm^{-1}, which overlaps the C=O absorptions at 1730-1740 cm^{-1} of ester linkage (not observables), and intense absorption bands at 1558 cm^{-1} (Amide II band, N-H bending of amide linkage formed between steroid hemisuccinates and FC).

The ^{1}H-NMR spectra of chitosan, FC, FC-vitamin and FC-steroid conjugates are shown in Figure 4.

The proton NMR spectrum of chitosan (Figure 4 (I) (a)) showed characteristic peaks at 2.10 ppm (s, methyl group of CH_3CO-), 3.19 ppm (s, 1H, H_b), 3.75 ppm (s, 1H, H_e), 3.80 ppm (s, 1H, H_{f*}) and 3.91 ppm (s, 3H, H_c+H_d+H_f) as reported for crab chitosans [29,30]. The ^{1}H-NMR of fructose chitosan was dominated by chitosan peaks; but it is observed a signal at 4.54 ppm (CH, C_a anomeric sugar proton of fructose-substituted glucosamine units).

The ^{1}H-NMR spectrum of FC-MSToc (Figure 4 (I) (c)) showed, in addition to chitosan peaks, signals at 0.65 ppm (methyl groups, 4'-CH_3+8'-CH_3+12'-CH_3), 1.21-1.23 ppm (methyl and methylene groups, 2-CH_3+H1' to H12'), 2.98 ppm (methylene groups, H14+H15 of succinyl moiety) and 4.16 ppm (CH-, C_a anomeric sugar proton of tocopheryl-substituted glucosamine units). FC-MSVitD2 (Figure 4 (I) (d)) presented peaks at ppm 0.94 ppm (methyl groups, H18+H26+H27), 1.10 ppm (methyl groups, H21+H28), 4.29/4.57 ppm (CH-, C_a anomeric sugar proton of ergocalciferol-substituted glucosamine and fructose-substituted glucosamine units, respectively).

The ^{1}H-NMR spectra of FC-steroid conjugates (Figure 4 (II) (a)-(c)) presented several peaks at 0.75/0.65/0.75 ppm (methyl group, H18 at MSD and MSDI31; H19 at MSS7), 0.78/0.83 ppm (methyl groups, H19+H27 at MSD and MSDI31 and H26+H27 at MSS7); 1.36-1.37/1.33 ppm (methyl group, H21 at MSD and MSS7), 2.58 ppm (methylene groups, H29+H30 and H31+H32 of succinyl moiety at MSD and MSS7, respectively), 4.32/4.43/4.27 ppm (CH-, C_a anomeric sugar proton of steroid-N-substituted glucosamine units at FC-MSD, FC-MSDI31 and FC-MSS7, respectively).

The wide-angle X-ray diffraction patterns of chitosan, fructose chitosan, FC-vitamin and FC-steroid conjugates are shown in Figure 5.

Chitosan presented low crystallinity, but defined peaks at 2θ 10.7° and 20.0° were observed (Figure 5). These peaks are attributed to the $(020)_h$ planes of the hydrated crystalline structure and the reflections of the hydrated polymorph respectively [31]. Fructose chitosan presents an X-rays pattern quite similar to chitosan with peaks at 10.1° and 20.0°, probably due to a very similar crystalline structure. However, the hydrophobically-modified FC conjugates showed several broad and intense peaks at 19.4° (FC-MSToc), 21.3° (FC-MSVitD2), 5.9° and 15.3° (FC-MSD), 12.5°, 14.7° and 17.4° (FC-MSDI31), 14.7° and 17.6° (FC-MSS7) (see Figure 5 and Table 1). The absence of intense peaks at 10.1° and 20.0° attributed to fructose chitosan is indicative of the absence of a pure FC crystalline phase. The characteristic narrow peaks of pure DL-α-tocopherol hemisuccinate, ergocalciferol hemisuccinate, diosgenin hemisuccinate and brassinosteroid hemisuccinates (MSDI31 and MSS7) were also absent (Table 1). Instead some broad peaks were observed, associated with the new crystalline phases of the prepared FC-vitamin and FC-steroid conjugates.

The DSC curves of chitosan, fructose chitosan, FC-vitamin and FC-steroid conjugates are shown in Figure 6. Thus, the DSC of parent chitosan (Figure 6 (I) (a)) showed two endothermic peaks at 170.4 °C and 187.0 °C, respectively. Their onset and completion temperatures are listed in Table 2, together with their associated peak enthalpy (ΔH). The total ΔH of these effects is 124.1 J/g. These endothermic effects must result mainly from the melting and dissociation of chitosan crystals, based on comparisons with reports for crab chitosans [28]. On the other hand, fructose chitosan presents three endothermic peaks at 207.5°C, 224.3 °C and 269.0 °C with an associated ΔH of 1741.5 J/g, 906.7 J/g and 51.4 J/g, respectively (see Table 2, related to decomposition of FC matrix). In this case, the total ΔH of these effects is 2699.6 J/g. Thus, dissociation and decomposition of FC chains appears to require much more energy than the needed in decomposition of chitosan chains.

The DSC of FC-MSToc (Figure 6 (I) (c)) exhibited two intense endothermic peaks at 173.4 °C and 224.8 °C, with related ΔH of 1431.4 J/g and 9853.6 J/g, respectively. The particularly high energy required (9853.6 J/g) in decomposition of FC-MSToc might be due to the aromatic stacking of tocopheryl fragments linked to different FC chains with the related stabilizing π–π interaction. The FC-MSVitD2 showed several endothermic peaks between 134-263 °C, with associated ΔH between 31-209 J/g. These peaks can result from the melting of tocopheryl-N-modified or ergocalciferol-N-modified FC, dissociation and decomposition of chitosan chains.

The DSC curves of FC-steroid conjugates (Figure 6 (II) (a)-(c)) present several intense endothermic peaks between 158–249 °C (see Table 2) with associated ΔH between 35–752 J/g. These peaks can result from the melting of FC-steroid crystals, dissociation and decomposition of chitosan molecular chains.

Drug delivery

The release profiles of DL-α-tocopherol and ergocalciferol from FC-MSToc and FC-MSVitD2 nanoparticles at 37 °C in PBS (pH 6.0), expressed as percent cumulative release against time, are presented in Figure 7 (I). Figure 7 (II) shows the release profiles of steroids from FC-steroid nanoparticles (FC-MSD, FC-MSDI31 and FC-MSS7) at 30 °C in PBS (pH 6.0). These studies were performed at pH 6.0 because acidic conditions are needed to achieve the hydrolysis of the ester linkage and the release of the vitamins and steroids. It is known that the interstitial space in cancer cells is acidic (pH ca. 6.5) due to increased excretion of lactic acid from the accelerated glucose metabolism [32], and particularly uptake of foreign bodies by endocytosis brings the FC nanoparticles to lysosomes with a pH of 5.0 [33]. On the other hand, vacuoles in vegetal cells also exhibit an acidic pH ca. 6.0 and some hydrolytic enzymes capable to degrade the FC-steroid nanoparticles that suffered endocytic uptake, thus releasing the brassinosteroids in the plants [34]. The *in vitro* drug release experiments were performed at two different temperatures (37 °C and 30 °C) because the FC-vitamin nanoparticles were intended for anticancer therapy, while the FC-steroid nanoparticles were aimed to agrochemical applications.

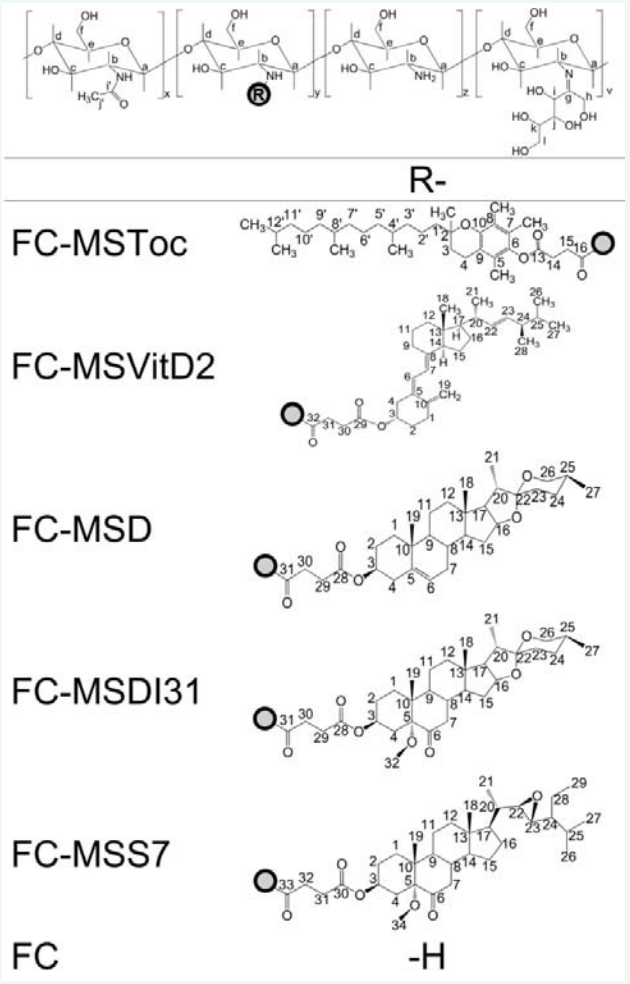

Figure 1 Structure of DL-α-tocopherol hemisuccinyl fructose chitosan (FC-MSToc), ergocalciferol hemisuccinyl fructose chitosan (FC-MSVitD2), diosgenin hemisuccinyl fructose chitosan (FC-MSD), DI-31 hemisuccinyl fructose chitosan (FC-MSDI31), S7 hemisuccinyl fructose chitosan (FC-MSS7) conjugates and fructose chitosan (FC).

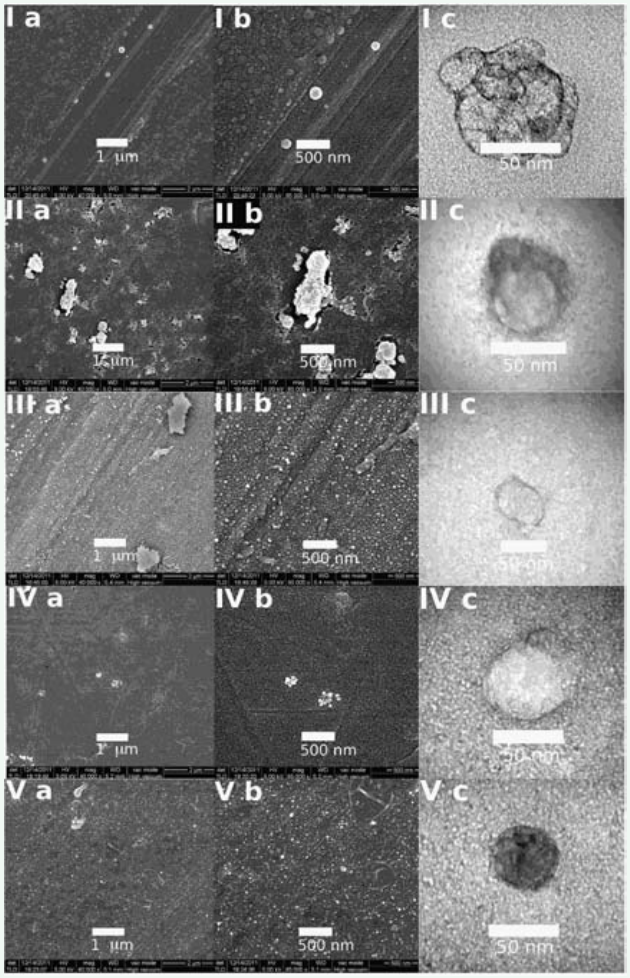

Figure 2 Scanning electron micrographs of: (I) FC-MSToc, (II) FC-MSVitD2, (III) FC-MSD, (IV) FC-MSDI31 and (V) FC-MSS7 nanoparticles at (a) 40000× and (b) 85000× magnifications, c) transmission electron micrograph at 100000× magnifications with negative staining (see Figure 1 for structures).

Table 1: WAXD peaks of chitosan, fructose chitosan, tocopheryl hemisuccinate, ergocalciferol hemisuccinate, steroid hemisuccinates and obtained FC conjugates (see Figure 1 for structures).

Samples	2 θ (degrees)								
CS	10.7	20.0	-	-	-	-	-	-	-
FC	10.1	20.0	-	-	-	-	-	-	-
MSToc	8.4	8.9	10.5	16.8	17.7	18.5	19.1	20.9	21.9
MSVitD2	16.1*	20.0	22.0*	26.0	31.4	38.1	38.4	42.0*	-
MSD	10.9	15.0	15.6	17.6	18.5	20.0*	21.7	22.9*	29.0*
MSDI31	4.3	6.2*	8.6*	11.8	12.4	14.5	17.3	18.5	20.9*
MSS7	4.2	8.7	11.6	12.1	14.4	17.1	17.6	20.8	25.1*
FC-MSToc	19.4	-	-	-	-	-	-	-	-
FC-MSVitD2	21.3	-	-	-	-	-	-	-	-
FC-MSD	5.9	9.1*	15.3	19.5*	-	-	-	-	-
FC-MSDI31	9.1*	12.5	14.7	17.4	20.4*	-	-	-	-
FC-MSS7	8.9*	9.6*	12.1*	14.7	17.6	21.2*	-	-	-

* stands for peaks of low intensity.

Table 2: Thermal properties and main endothermal effects of chitosan, fructose chitosan and obtained FC conjugates (see Figure 1 for structures).

Samples	Endotherm (ºC)			
	Onset	Peak	Completion	ΔH (J/g)
CS	167.2	170.4	174.1	3.5
	181.5	187.0	197.8	120.6
FC	178.0	207.5	210.8	1741.5
	210.8	224.3	242.4	906.7
	268.2	269.0	271.6	51.4
FC-MSToc	170.2	173.4	184.8	1431.4
	184.8	224.8	230.7	9853.6
FC-MSVitD2	132.2	134.4	136.0	31.1
	136.0	141.4	153.9	163.5
	153.9	159.0	179.1	209.1
	242.8	262.3	274.0	57.1
FC-MSD	154.6	158.0	159.7	42.0
	166.3	170.5	179.2	675.6
	179.2	187.1	196.3	284.7
FC-MSDI31	246.2	248.7	250.4	35.2
FC-MSS7	207.5	231.8	252.1	752.2

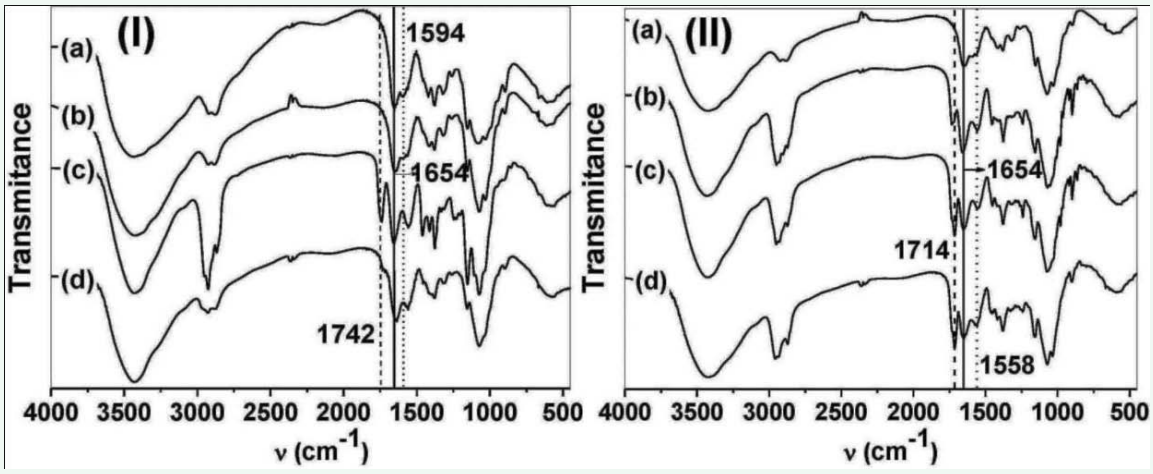

Figure 3 Infrared spectra of (I): (a) chitosan, (b) FC, (c) FC-MSToc and (d) FC-MSVitD2; (II): (a) FC, (b) FC-MSD, (c) FC-MSDI31 and (d) FC-MSS7 (see Figure 1 for structures).

The studied lipophilic vitamins showed sustained release with almost constant release rates (zero order kinetics) during the first 7-8 h. Release were not quantitative, reaching a cumulative release of 28 % (FC-MSToc) and 20% (FC-MSVitD2) after 96 h.

The steroid-N-modified fructose chitosan nanoparticles also presented sustained release with almost constant release rates during the first 8 h. Releases reached a 13% (FC-MSD), 61 % (FC-MSDI31) and 43% (FC-MSS7) after 96 h.

Agrochemical activity

Figure 8 shows the plant growth biological activity of the synthetic brassinosteroids DI31 and S7, fructose chitosan and FC-brassinosteroid nanoparticles in the radish cotyledons bioassay.

Plant growth stimulator activities of the synthetic brassinosteroids DI31 and S7 are quite similar, showing best results at 10^{-3} and 10^{-4} mg mL^{-1} concentrations, but almost a doubled cotyledons weight was reached as compared to control with the lowest concentrations (10^{-6} and 10^{-7} mg mL^{-1}). Fructose chitosan exerts a comparable growth stimulator effect at higher concentrations (10^{-1} to 10^{-4} mg mL^{-1}), but no activity is observed at low concentrations (10^{-5} to 10^{-7} mg mL^{-1}).

The studied FC-MSDI31 and FC-MSS7 nanoparticles in aqueous solution presented very good and almost constant stimulatory activities at all concentrations (weight increased approximately four times compared to control). A doubled of cotyledons weight increase was reached when compared to pure brassinosteroids (DI31 and S7) at lowest concentrations (10^{-6} and 10^{-7} mg mL^{-1}), which might be due to the controlled release of exogenous brassinosteroid analogues (DI31 and S7) in the required nanomolar concentrations for a stimulatory growth effect in the radish cotyledons [21,35].

CONCLUSIONS

Synthesized fructose chitosan was covalently linked to tocopherol, ergocalciferol and different steroids with

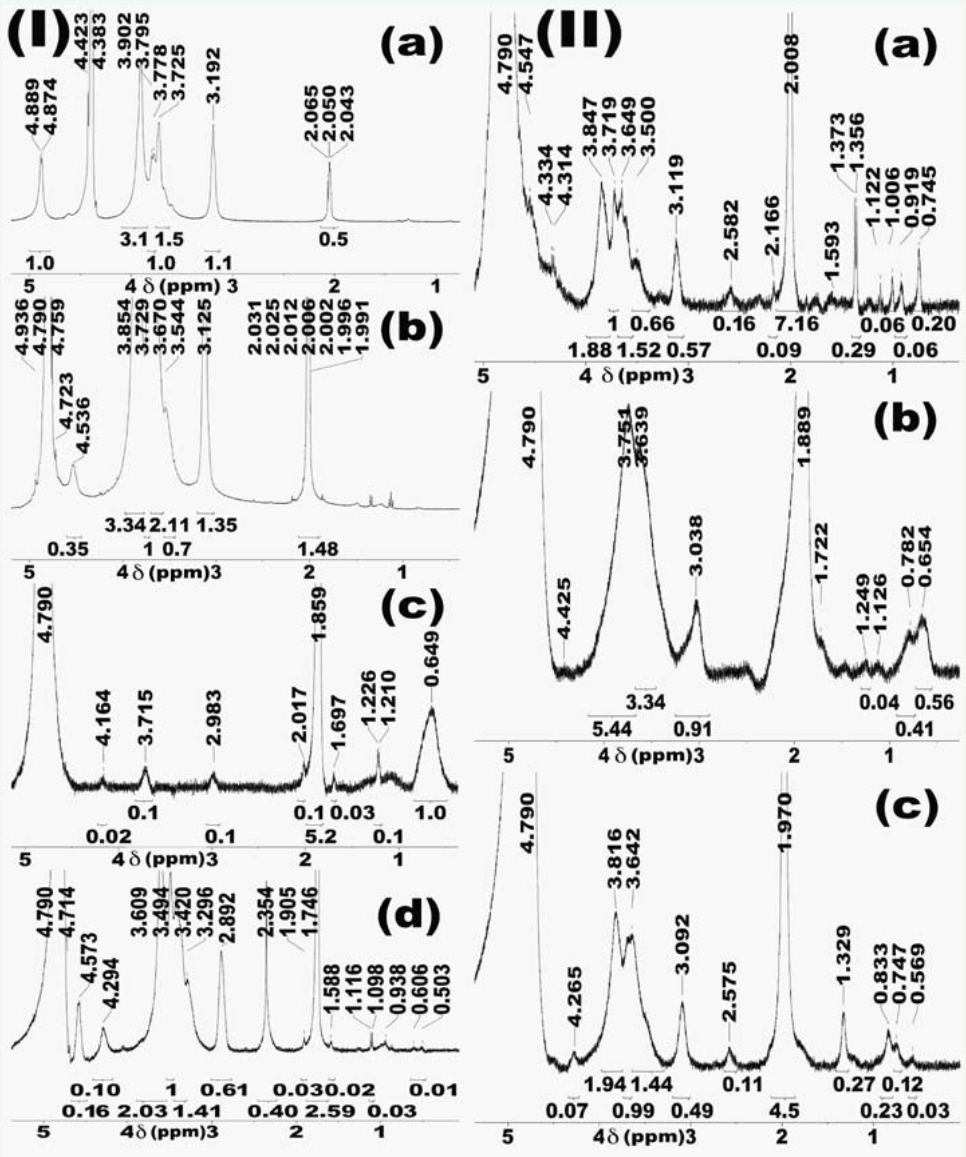

Figure 4 Proton NMR spectra of (I): (a) chitosan and (b) FC at 8 mg mL-1 in D2O; (c) FC-MSToc and (d) FC-MSVitD2 at 25 mg mL-1 in CD3COOD/D2O (1:3) at 25 °C; (II): (a) FC-MSD, (b) FC-MSDI31 and (c) FC-MSS7 at 25 mg mL-1 in CD3COOD/D2O (1:3) at 25 °C (see Figure 1 for structures).

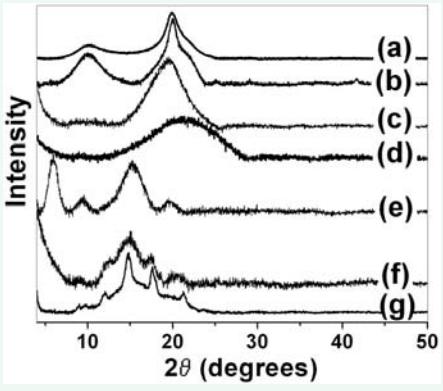

Figure 5 Wide-angle X-ray diffraction patterns of: (a) chitosan, (b) FC, (c) FC-MSToc, (d) FC-MSVitD2, (e) FC-MSD, (f) FC-MSDI31 and (g) FC-MSS7 (see Figure 1 for structures).

agrochemical and potential anticancer activity for their controlled release, as confirmed by FTIR and proton NMR spectroscopies. Hydrophobic modification of fructose chitosan ranged from 5.5 to 39.0 mol-%. These FC conjugates formed self-assembled nanoparticles in aqueous solution upon sonication and released the linked vitamins and steroids in aqueous acidic medium (PBS, pH 6.0) with almost constant rates during the first 7-8 h. The brassinosteroid-N-modified fructose chitosan nanoparticles showed increased agrochemical activities as compared to the pure brassinosteroids. These results indicate that hydrophobically-modified fructose chitosan nanoparticles are efficient pH dependent drug delivery systems for the sustained release of lipophilic vitamins and agrochemicals.

ACKNOWLEDGEMENTS

The authors wish to thank the Erasmus Mundus for a research grant to Javier Pérez Quiñones. Prof. Jacques Chevallier and Ms.

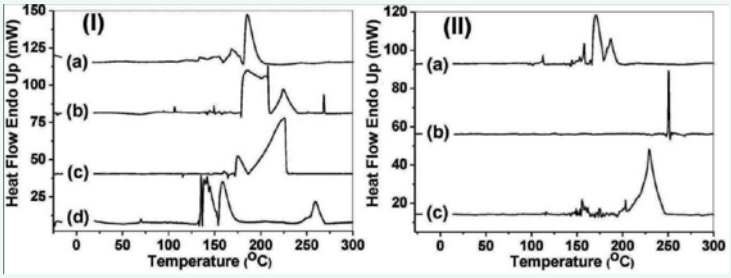

Figure 6 DSC Curves of (I): (a) chitosan, (b) FC, (c) FC-MSToc and (d) FC-MSVitD2; (II): (a) FC-MSD, (b) FC-MSDI31 and (c) FC-MSS7 (see Figure 1 for structures).

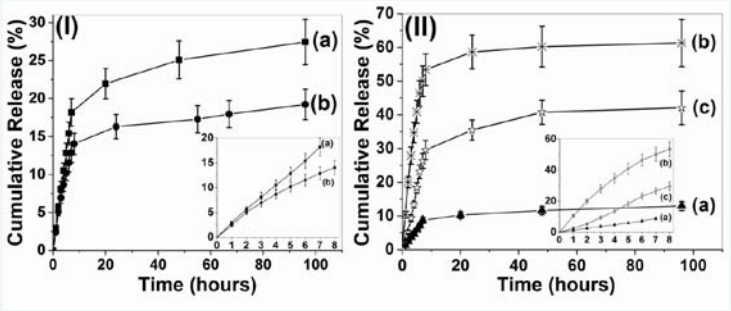

Figure 7 In vitro release profile of (I): (a) FC-MSToc and (b) FC-MSVitD2 at 37 ± 2 °C in PBS (pH= 6.0); (II): (a) FC-MSD, (b) FC-MSDI31 and (c) FC-MSS7 at 30 °C in PBS (pH = 6.0) (see Figure 1 for structures).

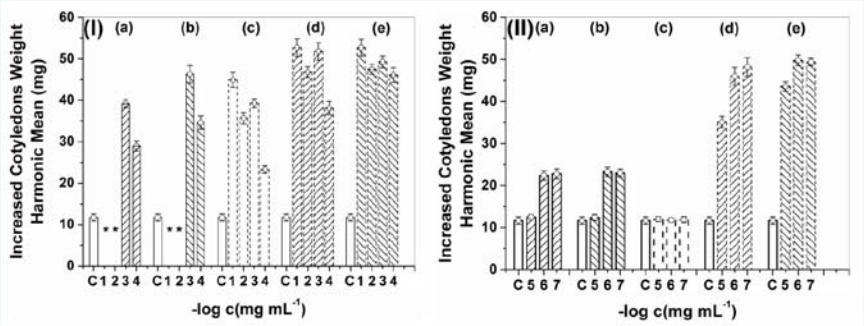

Figure 8 Agrochemical activity of (I): Control (C), (a) DI31, (b) S7, (c) FC, (d) FC-MSDI31, (e) FC-MSS7 at 25 °C in concentrations of 10^{-1} to 10^{-4} mg mL^{-1}; (II): Control (C), (a) DI31, (b) S7, (c) FC, (d) FC-MSDI31, (e) FC-MSS7 at 25 °C in concentrations of 10^{-5} to 10^{-7} mg mL^{-1}. (*) Not measured because cotyledons died as result of high ethanol content. Data represents the mean ± standard deviation (n = 3) (see Figure 1 for structures).

Karen E. Thomsen are acknowledged by electron microscopy measurements at Aarhus University, Denmark. Prof. Dr. Jens-Erik Jørgensen is acknowledged for X-ray diffraction measurements in Institut for Kemi at Aarhus University, Denmark. Prof. Dr. Claudia Schmidt is gratefully acknowledged for helpful revision of the manuscript and elemental analysis and DSC measurements in Department of Chemistry, University of Paderborn, Germany.

REFERENCES

1. Muzzarelli RAA. Chitin nanostructures in living organisms. In: S. Gupta, editor. Chitin: Formation and Diagenesis. Dordrecht: Springer. 2011; 1-34.

2. Ahsan SM, Thomas M, Reddy KK, Sooraparaju SG, Asthana A, Bhatnagar I. Chitosan as biomaterial in drug delivery and tissue engineering. Int J Biol Macromol. 2017.

3. Raafat D, Sahl HG. Chitosan and its antimicrobial potential – a critical literature survey. Microb Biotechnol. 2009; 2: 186-201.

4. Malerba M, Cerana R. Chitosan Effects on Plant Systems. Int J Mol Sci. 2016; 17: 996-1011.

5. Jing-Mou Y, Li-Yan Q, Yi, J, Yong-Jie L. Self-aggregated nanoparticles of cholesterol-modified glycol chitosan conjugate: Preparation, characterization, and preliminary assessment as a new drug delivery carrier. Eur Polym J. 2008; 44: 555-565.

6. Pereira P, Pedrosa SS, Correia A, Lima CF, Olmedo MP, González-Fernández A, et al. Biocompatibility of a self-assembled glycol chitosan nanogel. Toxicol in Vitro. 2015; 29: 638-646.

7. Chung YC, Li CF, Tsai CF. Preparation and characterization of water-soluble chitosan produced by Maillard reaction. Fisheries Sci. 2006; 72: 1096-1103.

8. Chen CC, Chung YC, Kuo CL. Preparation and important functional properties of water-soluble chitosan produced through Maillard reaction. Bioresour Technol. 2005; 96: 1473-1482.

9. Aiba S, Chirachanchai S, Phongying S. A novel soft and cotton-like chitosan-sugar nanoscaffold. Biopolymers. 2006; 83: 280-288.

10. Bell TD, Burnett-Bowie SAM, Demay MB. The biology and pathology of vitamin D control in bone. J Cell Biochem. 2010; 111: 7-13.

11. Rolewski P, Siger A, Nogala-Kalucka M, Polewski K. Evaluation of antioxidant activity of alpha-tocopherol and quercetin during oxidation of phosphatidylcholine using chemiluminescent detection of lipid hydroperoxides. Pol J Food Nutr Sci. 2009; 59: 123-127.

12. Nimse SB, Pal D. Free radicals, natural antioxidants, and their reaction mechanisms. RSC Adv. 2015; 5: 27986-28006.

13. Kulling PM, Olson KC, Olson TL, Feith DJ, Loughran TP. Vitamin D in hematological disorders and malignancies. Eur J Haematol. 2016; 98: 187-197.

14. Gupta SD, Patel M, Wahler J, Bak MJ, Wall BA, Lee MJ, et al. Differential gene regulation and tumor inhibitory activities of alpha-, delta- and gamma-tocopherols in estrogen-mediated mammary carcinogenesis. Cancer Prev Res (Phila). 2017.

15. Aumsuwan P, Khan SI, Khan IA, Ali Z, Avula B, Walker LA, Shariat-Madar Z, et al. The anticancer potential of steroidal saponin, dioscin, isolated from wild yam (*Dioscorea villosa*) root extract in invasive human breast cancer cell line MDA-MB-231 in vitro. Arch Biochem Biophys. 2016; 591: 98-110.

16. Alché LE, Berra A, Galagovsky LR, Michelini FM, Ramírez JA. In vitro and in vivo antiherpetic activity of three new synthetic brassinosteroid analogues. Steroids. 2004; 69: 713-720.

17. Rivera DG, León F, Coll F, Davison GP. Novel 5-hydroxyspirostan-6-ones ecdysteroid antagonists: Synthesis and biological testing. Steroids. 2006; 71: 1-11.

18. Serrano YC, Fernández RR, Pineda FR, Pelegrín LTS, Fernández DG, Cepero MCG. Synergistic effect of low doses of X-rays and Biobras-16 on yield and its components in tomato (*Solanum lycopersicum L.*) plants. Am J Biosci Bioeng. 2015; 3: 197-202.

19. Akram NA, Arteca RN, Ashraf M, Foolad MR. The Physiological, Biochemical and Molecular Roles of Brassinosteroids and Salicylic Acid in Plant Processes and Salt Tolerance. CRC Crit Rev Plant Sci. 2010; 29: 162-190.

20. Bajguz A, Hayat S. Effects of brassinosteroids on the plant responses to environmental stresses. Plant Physiol Bioch. 2009; 47: 1-8.

21. Sasse JM. Physiological Actions of Brassinosteroids: An Update. J Plant Growth Regul. 2003; 22: 276-288.

22. Quiñones JP, Szopko R, Schmidt C, Covas CP. Novel drug delivery systems: Chitosan conjugates covalently attached to steroids with potential anticancer and agrochemical activity. Carbohydr Polym. 2011; 84: 858-864.

23. Kean T, Thanou M. Biodegradation, biodistribution and toxicity of chitosan. Adv Drug Deliv Rev. 2010; 62: 3-11.

24. Abe T, Hasunuma K, Kurokawa M. Vitamin E orotate and a method of producing the same. 1976. US: 3944550.

25. Alonso-Becerra E, Bernardo-Otero Y, Coll-Manchado F, Guerra-Martínez F, Martínez-Massanet G, Pérez-Martínez C. Synthesis and biological activity of epoxy analogues of 3-dehydroteasterone. J Chem Res. 2007; 5: 268-271.

26. Honary S, Zahir F. Effect of zeta potential on the properties of nano-drug delivery systems - A review (Part 2). Trop J Pharm Res. 2013; 12: 265-273.

27. El-Marakby EM, Hathout RM, Taha I, Mansour S, Mortada ND. A Novel serum-stable liver targeted cytotoxic system using valerate-conjugated chitosan nanoparticles surface decorated glycyrrhizin. Int J Pharm. 2017; 525: 123-138.

28. Quiñones JP, García YC, Curiel H, Covas CP. Microspheres of chitosan for controlled delivery of brassinosteroids with biological activity as agrochemicals. Carbohydr Polym. 2010; 80: 915-921.

29. Berrada M, Buschmann MD, Gupta A, Lavertu M, Rodrigues A, Serreqi AN, et al. A validated 1H NMR method for the determination of the degree of deacetylation of chitosan. J Pharm Biomed Anal. 2003; 32: 1149-1158.

30. Hirai A, Nakajima A, Odani H. Determination of degree of deacetylation of chitosan by 1 H NMR spectroscopy. Polym Bull (Berl). 1991; 26: 87-94.

31. David L, Domard A, Lucas J-M, Osorio-Madrazo A, Peniche-Covas C, Trombotto S. Kinetics Study of the Solid-State Acid Hydrolysis of Chitosan: Evolution of the Crystallinity and Macromolecular Structure. Biomacromolecules. 2010; 11: 1376-1386.

32. Kato Y, Ozawa S, Miyamoto C, Maehata Y, Suzuki A, Maeda T, et al. Acidic extracellular microenvironment and cancer. Cancer Cell Int. 2013; 13: 1-8.

33. Duncan R, Richardson CW. Endocytosis and intracellular trafficking asgateways for nanomedicine delivery: Opportunities and challenges. Mol Pharm. 2012; 9: 2380-2402.

34. Fan L, Li R, Pan J, Ding Z, Lin J. Endocytosis and its regulation in plants. Trends Plant Sci. 2015; 20: 388-397.

35. Liu J, Zhang D, Sun X, Ding T, Lei B, Zhang C. Structure-activity relationship of brassinosterois and their agricultural practical usages. Steroids. 2017; 124: 1-17.

Cite this article

Quiñones JP, Brüggemann O, Covas CP (2017) Fructose Chitosan Based Self-Assembled Nanoparticles for Sustained Release of Vitamins and Steroids. JSM Nanotechnol Nanomed 5(3): 1056.